

# Quaternary upper ocean thermal gradient variations in the South China Sea: Implications for east Asian monsoon climate

Jun Tian,<sup>1,2</sup> Pinxian Wang,<sup>1</sup> Ronghua Chen,<sup>3</sup> and Xinrong Cheng<sup>1</sup>

Received 17 November 2004; revised 7 June 2005; accepted 29 June 2005; published 26 October 2005.

[1] The east Asian monsoon climate has an overwhelming influence on local climatic conditions of the South China Sea (SCS). Here we present results from a 3-year study of modern sediment traps from the central SCS in which the percentage of opal, the fluxes of *Pulleniatina obliquiloculata* and *Globigerinoides ruber*, the organic carbon flux, and primary productivity all show highest values during winter when the mixed layer depth is deepest. The  $\delta^{18}\text{O}$  difference ( $\Delta\delta^{18}\text{O}_{(P-G)}$ ) between the subsurface dwelling *P. obliquiloculata* and the mixed layer dwelling *G. ruber* in core top samples from 12 piston cores and one Ocean Drilling Program (ODP) site in the SCS is large,  $\sim 0.6\%$  in a cold eddy area with a shallow mixed layer off Vietnam, but is reduced in deep mixed layer settings lacking cold eddies. We also present 1.56 Myr-long isotope records of *G. ruber* and *P. obliquiloculata* from ODP site 1143 in the southern SCS that reveal upper ocean thermal gradient variations during the Quaternary. Lower  $\Delta\delta^{18}\text{O}_{(P-G)}$  values indicate increased mixed layer depths over most glacial episodes, likely due to stronger winter monsoon winds. In contrast, higher  $\Delta\delta^{18}\text{O}_{(P-G)}$  values during interglacial intervals suggest decreased mixed layer depths and thus weaker winter monsoon winds. Comparisons of  $\Delta\delta^{18}\text{O}_{(P-G)}$  with the percentage of *P. obliquiloculata* at site 1143 and the percentage of herbs and opal flux at site 1144 demonstrate that glacial-interglacial variations were strongly influenced by stronger and weaker east Asian winter monsoons during glacials and interglacials, respectively. Therefore the upper ocean thermal gradient variations in the SCS have been consistently affected by the east Asian winter monsoon since at least the beginning of the Pleistocene.

**Citation:** Tian, J., P. Wang, R. Chen, and X. Cheng (2005), Quaternary upper ocean thermal gradient variations in the South China Sea: Implications for east Asian monsoon climate, *Paleoceanography*, 20, PA4007, doi:10.1029/2004PA001115.

## 1. Introduction

[2] The east Asian monsoon is the primary modulator of local environmental conditions over east Asia. Differential heating of the northwest Pacific and of the Asian landmass causes a seasonal reversal of monsoon winds that dominate seasonal surface circulation patterns over the South China Sea (SCS). From November to March, the winter Asian high-pressure system brings strong winds from the northeast, leading to a cyclonic surface circulation in the SCS; from June to September, the summer monsoon winds blow from the southwest, causing anticyclonicity in surface circulation in the southern basin [Wyrki, 1961].

[3] Long-term changes in the east Asian monsoons during the Quaternary have been recorded in great detail in loess-paleosol sequences from central Asia [Porter and An, 1995]. Several proxies, such as grain size and Al fluxes, and magnetic susceptibility and Rr/Sr ratio, reveal glacial/interglacial fluctuations of the east Asian winter and sum-

mer monsoons, respectively [Porter *et al.*, 1992; Ding *et al.*, 1992]. However, the use of marine indices to study long-term east Asian monsoon variations has not kept pace with the use of terrestrial proxies. One obvious reason is that oceanic deposition is much more complex than terrestrial eolian deposition. Marine sedimentation usually involves physical, biological, and/or chemical processes, making marine proxies of climate change associated not with one unique climatic variable but with the integration of several variables. Therefore, in order to reveal long-term variations of the east Asian monsoon from deep sea sediments of the SCS, it is better to utilize multiproxy records with the support of evidence from modern hydrological features and from core top and sediment trap analyses. Here we present results from core top samples and a 1.56 Myr-long isotope record of the mixed layer dwelling foraminiferal species *Globigerinoides ruber* and the subsurface dwelling species *Pulleniatina obliquiloculata* from Ocean Drilling Program (ODP) site 1143 in the southern SCS (Figure 1a) to reveal the upper ocean thermal gradient variations during the Pleistocene. Combined with other proxy records, we will explore the long-term evolution of the east Asian monsoon climate system.

## 2. Materials and Methods

[4] To extract paleoceanographic features from core top samples in the SCS, we selected two piston cores within

<sup>1</sup>State Key Laboratory of Marine Geology, Tongji University, Shanghai, China.

<sup>2</sup>Institute of Geology and Geophysics, Chinese Academy of Sciences, Beijing, China.

<sup>3</sup>Key Laboratory of Submarine Geosciences of State Oceanic Administration, Hangzhou, China.

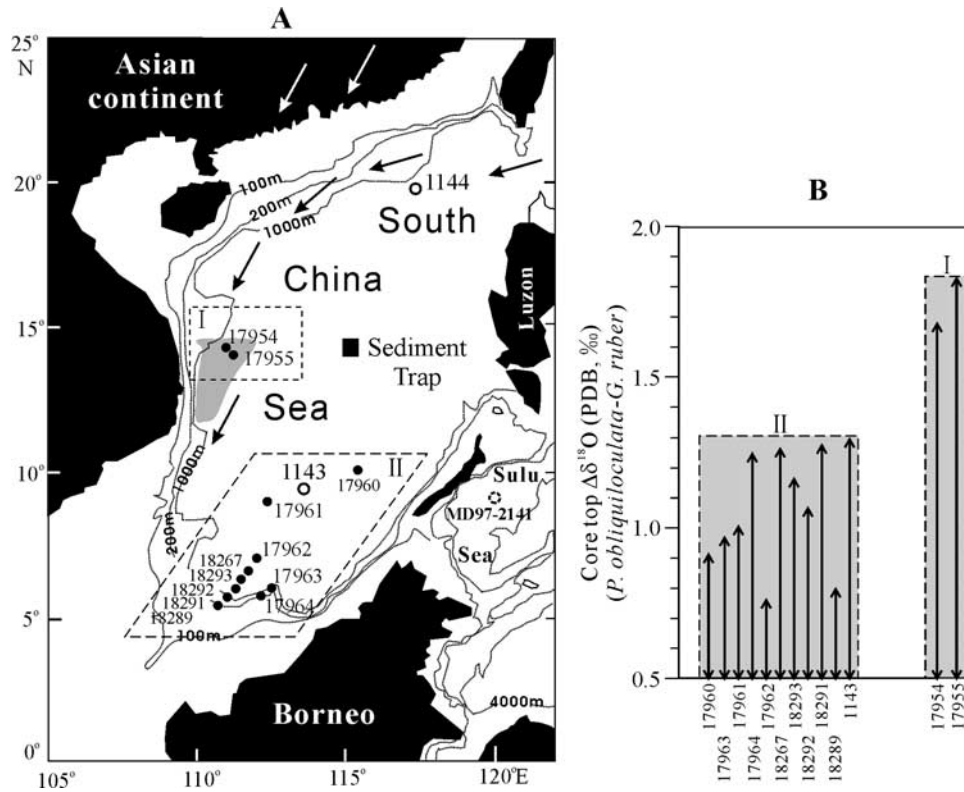


**Figure 1.** (a) Locations of 12 piston cores (solid circles) and two drilled sites (large open circles) in the South China Sea. The open dashed circle denotes the IMAGES core MD97-2141 in the Sulu Sea [Oppo *et al.*, 2003]. White arrows denote the direction of the east Asian winter monsoon winds. Black arrows denote the winter monsoon-induced sea surface circulation in the SCS. The solid square denotes the location of the sediment trap in the central SCS. Core group 1, confined to the dashed square, includes 17954 and 17955, which are within the cold eddy areas off Vietnam (shaded area). Core group 2, confined to the dashed parallelogram, includes site localities without cold eddies. (b) Core top  $\delta^{18}\text{O}$  differences between *P. obliquiloculata* and *G. ruber*. Core top data for 17954 and 17955 are from Grothmann [1996], used by permission from Michael Sarnthein of Kiel University, Kiel, Germany. The arrow range denotes the  $\delta^{18}\text{O}$  difference of each individual core top sample. The core top samples were obtained during the SONNE-95 cruise [Sarnthein *et al.*, 1994] and the SONNE-115 cruise [Stattegger *et al.*, 1997].

the cold eddy area off Vietnam and 10 piston cores and one Ocean Drilling Program (ODP) site within the non-cold eddy areas in the southern SCS (Figure 1a). Stable oxygen and carbon isotopes were measured on the thermocline dwelling species *P. obliquiloculata* and the mixed layer dwelling species *G. ruber* with a size of 0.25–0.35 mm from all the core top samples (4 individuals for each species). *G. ruber* is a mixed layer dweller that lives at depths between ~30–60 m in the upper mixed layer of the modern ocean [Hemleben *et al.*, 1989], while *P. obliquiloculata* is a thermocline dweller that is constrained to the top of the thermocline or the bottom of the mixed layer in the western Pacific [Pflaumann and Jian, 1999]. Samples from the cold eddy area (Figure 1b, group 1, cores 17954 and 17955) [Grothmann, 1996] were measured in the Isotope Analysis Laboratory of Kiel University and the rest (Figure 1B, group 2) were measured in the State Key Laboratory of Marine Geology, Tongji University. Although the two laboratories are not directly intercalibrated, they utilize the same devices for isotopic analysis

(Finnigan MAT252 and Finnigan automatic carbonate device (Kiel III)) and have similar analytical precision. The standard deviations of the laboratories at Tongji University and Kiel University are 0.07‰ for  $\delta^{18}\text{O}$  and 0.04‰ for  $\delta^{13}\text{C}$ .

[5] For stable isotope measurements of ODP site 1143, samples were selected from the upper 75.62 m of the core with a spacing of 10 cm. The thickness of each sample is 2 cm. Well preserved specimens of *G. ruber* and *P. obliquiloculata* with a diameter of 0.25–0.35 mm (4 individuals) were picked and used. Sample preparation and stable isotope analyses follow standard procedures summarized in our previous studies [Tian *et al.*, 2002, 2003].

[6] The age model is based on the benthic  $\delta^{18}\text{O}$  record of site 1143 tuned to obliquity and precession using the Laskar [1990] (1, 0) solution [Tian *et al.*, 2002]. After tuning, the depth of 75.62 m of site 1143 corresponds to an age of 1.56 Ma and the average temporal resolution of the records is ~2 kyr. For each sample of site 1143, in addition to the benthic foraminifers, we selected surface and subsurface

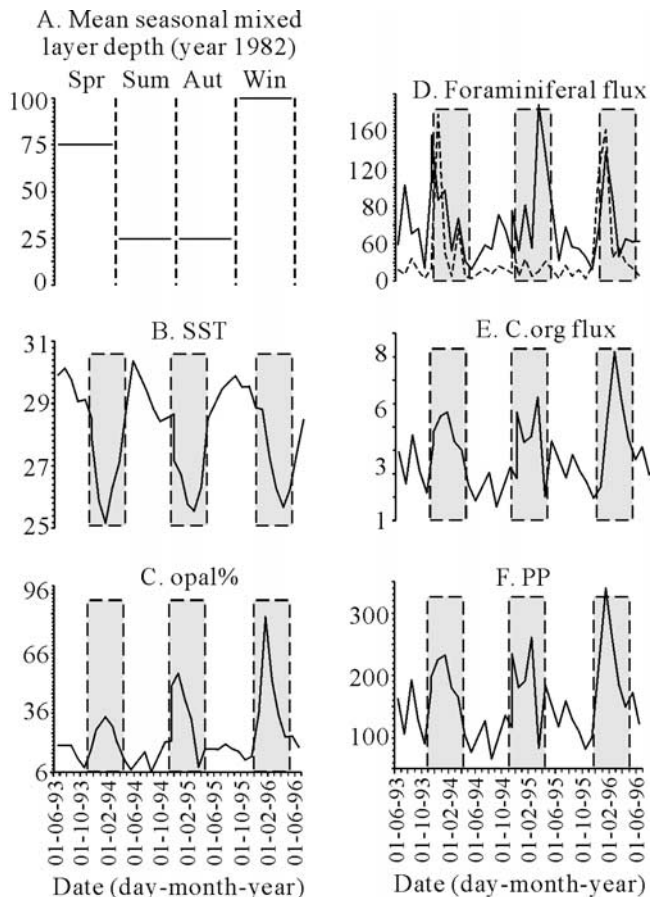


**Figure 2.** Modern observations in the central SCS: (a) average seasonal mixed layer depth of the South China Sea (m), integrated from the data of *Levitus* [1982]; (b) sea surface temperature; (c) percentage of opal; (d) *P. obliquiloculata* (dashed line) and *G. ruber* (solid line) flux (individuals  $\text{m}^{-2} \text{d}^{-1}$ ); (e) organic carbon flux ( $\text{mg m}^{-2} \text{d}^{-1}$ ); and (f) primary productivity ( $\text{mg m}^{-2} \text{d}^{-1}$ ). Data from *B* and *F* are our original sediment trap data in the central SCS.

planktonic foraminifers to measure the oxygen and carbon isotopes.

### 3. Results

#### 3.1. Reconstruction of Southern SCS Hydrography

[7] Previous studies have demonstrated that the  $\delta^{18}\text{O}$  difference between planktonic subsurface dwelling species such as *P. obliquiloculata* and surface dwelling species such as *G. ruber* can be used to indicate the relative depth of the tropical mixed layer [Ravelo and Shackleton, 1995]. Large  $\delta^{18}\text{O}$  differences between subsurface and surface species usually indicate a shallow thermocline with a large temperature range in the photic zone, where small  $\delta^{18}\text{O}$  differences often result from a deepened thermocline with a narrow temperature range [Ravelo and Shackleton, 1995]. For example, in the modern tropical Pacific, the thermocline is deep in the west but shallow in the east. The subsurface to

surface foraminiferal  $\delta^{18}\text{O}$  differences in core top samples are smaller (1.0‰) in the west Pacific but large (1.9‰) in the east Pacific, corresponding to the deep and shallow thermoclines in these two Pacific sectors respectively [Billups *et al.*, 1999]. In the equatorial Atlantic, the subsurface to surface foraminiferal  $\delta^{18}\text{O}$  differences in core top samples are smaller (0.9‰) in the west with a deep thermocline but large (1.4‰) in the east with a shallow thermocline [Billups *et al.*, 1999]. By using  $\delta^{18}\text{O}$  differences between the subsurface *G. tumida* and the surface dwelling species *G. sacculifer*, Billups *et al.* [1999] constructed the upper ocean thermal gradient variations at the open west Pacific ODP site 806 between 5 and 3 Ma. The consistently small  $\delta^{18}\text{O}$  differences led these authors to suggest that the thermal gradient in the photic zone remained small and the mixed layer remained deep during the early Pliocene at the site 806 locality.

[8] In the SCS, modern observations and numerical simulations have found that cold eddies driven by coastal upwelling occur during winter off the northwest shore of Luzon island (16–19°N), and in the summer off Vietnam (12–14°N) [Shaw, 1996; Yang and Liu, 1998]. The cold eddies lead to a shallower thermocline in these upwelling areas than in other nonupwelling areas of the SCS [Shaw, 1996]. The isotopic measurements of the core top samples (Figure 1b) show smaller  $\delta^{18}\text{O}$  differences of 0.76‰ to 1.38‰ between *P. obliquiloculata* and *G. ruber*, with an average of 1.09‰, from areas without cold eddies, and much larger  $\delta^{18}\text{O}$  differences of 1.68‰ and 1.83‰, or 1.76‰ on average, from cold eddy-influenced areas. These results imply that, in the SCS, the photic zone temperature gradient is larger in the cold eddy areas with a shallow thermocline and smaller in the non-cold eddy areas with a deep thermocline. The  $\delta^{18}\text{O}$  differences between the thermocline species *P. obliquiloculata* and mixed layer species *G. ruber*, hereinafter referred to as  $\Delta\delta^{18}\text{O}_{(P-G)}$ , thus can be used to indicate glacial/interglacial thermal gradient variations in the SCS, with large  $\Delta\delta^{18}\text{O}_{(P-G)}$  values implying decreased mixed layer depth, and vice versa.

[9] In the modern SCS, winter is the season when the average seasonal mixed layer reaches its maximum depth of about 100 m, lasting from December to March [Wang *et al.*, 2001; Levitus, 1982] (Figure 2a). Meanwhile, the mean seasonal SST (sea surface temperature) declines to its lowest point (Figure 2b). By using the *Levitus and Boyer* [1994] data, Wang *et al.* [2001] found that the upper ocean of the SCS became more ventilated during winter times. The low-latitude ocean is strongly stratified by the warmth of its surface water [Sigman *et al.*, 2004]. In the SCS during winter, the decreased SST may help make the upper ocean less stratified. Under the influence of the strong east Asian winter monsoon winds, mixing of the upper ocean of the SCS reaches its maximum and the mixed layer expands to its deepest depth about 100 m within an annual cycle.

[10] Newly obtained sediment trap data (1993–1996, 14°36.2'N, 115°07.1'E, 1208 m; refer to Wiesner *et al.* [1996] for details of trap deployment) reveal that several paleoclimate proxies, including the percentage of opal, *P. obliquiloculata* and *G. ruber* flux, organic carbon flux and primary productivity, all exhibit higher values during winter (from December to March) than during the other

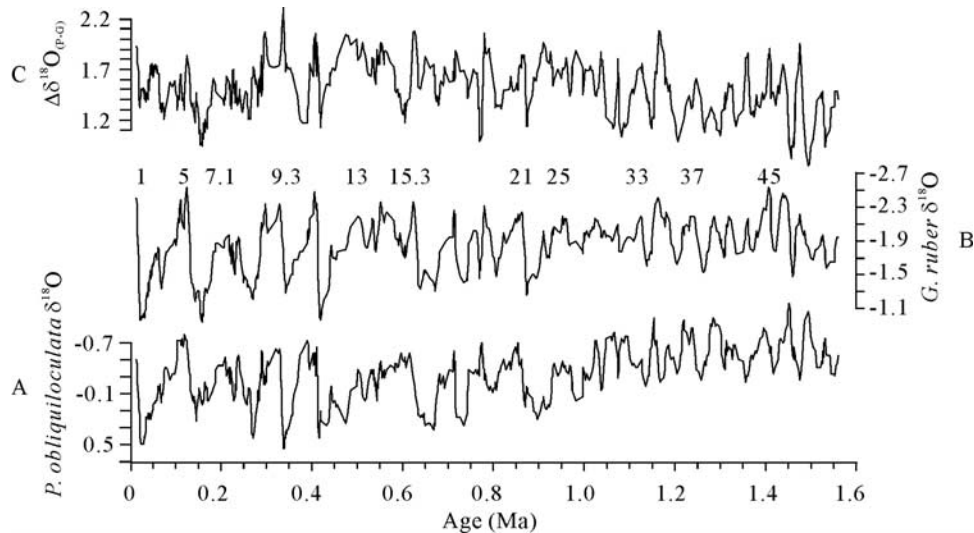


**Figure 3.** Foraminiferal isotopic records from the South China Sea: (a) site 1143 subsurface water species *P. obliquiloculata*  $\delta^{18}\text{O}$  (Pee Dee Belemnite (PDB), ‰, 3-point Gaussian smoothing, 0–1.56 Ma), (b) site 1143 surface water species *G. ruber*  $\delta^{18}\text{O}$  (PDB, ‰, 3-point Gaussian smoothing, 0–1.56 Ma), and (c) site 1143  $\Delta\delta^{18}\text{O}_{(P-G)}$  (*P. obliquiloculata*  $\delta^{18}\text{O}$  minus *G. ruber*  $\delta^{18}\text{O}$ ) (PDB, ‰, 3-point Gaussian smoothing, 0–1.56 Ma).

seasons (Figures 2c, 2d, 2e, and 2f). In the northern SCS near the Luzon strait, core top analyses reveal that the percent of *P. obliquiloculata* rapidly decreases along the flow direction of the winter surface current which is apparently driven by the east Asian winter monsoon [Pflaumann and Jian, 1999].

### 3.2. Glacial-Interglacial Variability of the Thermal Gradient in the Southern SCS

[11] Figures 3a, 3b, and 3c, respectively, illustrate glacial-interglacial fluctuations of  $\delta^{18}\text{O}_{P. obliquiloculata}$ ,  $\delta^{18}\text{O}_{G. ruber}$  and  $\Delta\delta^{18}\text{O}_{(P-G)}$  ( $\delta^{18}\text{O}_{P. obliquiloculata}$  minus  $\delta^{18}\text{O}_{G. ruber}$ ) recorded at site 1143 over the last 1.56 Myr after 3-point Gaussian smoothing. Smoothing removes abnormal spikes that can result from either extreme isotope values or small isotopic structure differences especially at steep transitions from glacial to interglacial stages. In general,  $\Delta\delta^{18}\text{O}_{(P-G)}$  values are reduced 0.5–1.0‰ during glacials or stadials compared to the adjoining interglacials or interstadials, suggesting that the thermal gradient remained low and the mixed layer was deep during glacial and stadial periods. In contrast, during interglacial or interstadial periods, large  $\Delta\delta^{18}\text{O}_{(P-G)}$  values imply an increased thermal gradient and a deeper mixed layer. Exceptions to this general pattern are few, including relatively high  $\Delta\delta^{18}\text{O}_{(P-G)}$  values for marine isotope stages (MIS) 16 and relatively low values for MIS 17.

### 3.3. Comparison of *G. Ruber* $\delta^{18}\text{O}$ Between South China Sea and Sulu Sea

[12] Sulu Sea is the closest adjacent sea to the southern SCS, and is a semienclosed basin that exchanges water with the SCS through the Mindoro Passage, the deepest connection (420 m) between the two. The Sulu Sea is located between the SCS and the Western Pacific Warm Pool

(WPWP), two regions that exhibit opposite responses to ENSO variability [Oppo *et al.*, 2003]. Modern observations reveal that the seasonal surface waters of the Sulu Sea are saltier than those of the southern SCS, whereas the seasonal sea surface temperatures in both basins are quite similar [Levitus and Boyer, 1994]. These hydrological characteristics of the two basins should result in *G. ruber*  $\delta^{18}\text{O}$  from SCS having predictably lower values than from the Sulu Sea. Figure 4 shows a comparison of *G. ruber*  $\delta^{18}\text{O}$  between the SCS and Sulu Sea. In general, over the past 400 kyr, both glacial and interglacial *G. ruber*  $\delta^{18}\text{O}$  values from site 1143 in the southern SCS were indeed lower by  $\sim 0.3$ – $0.5$ ‰ than those from the International Marine Past Global Changes Study (IMAGES) core MD97-2141 in the Sulu Sea. Furthermore, from stage 6 to the Holocene, the glacial/interglacial (G-I) amplitude of the *G. ruber*  $\delta^{18}\text{O}$  at site 1143 is also larger than that of core MD97-2141 (Figure 4). Previous work in the Sulu Sea has shown that the G-I amplitude of planktonic  $\delta^{18}\text{O}$  over the past 150 kyr was similar to that due to changes in ice volume alone, and that the low planktonic  $\delta^{18}\text{O}$  amplitude on G-I timescales in the Sulu Sea was due to the minimal sea surface temperature (SST) changes [Linsley, 1996]. This conclusion is consistent with results of SST reconstructions since the last glacial maximum (LGM) in both the Sulu Sea and SCS. The warming across the recent deglaciation in the southern SCS was  $\sim 3^\circ\text{C}$  on the basis of alkenone paleothermometry from cores 18252-3 and 18287-3 [Kienast *et al.*, 2001], whereas the warming from the LGM to the Holocene in the Sulu Sea was only  $\sim 2.3^\circ\text{C}$  on the basis of Mg/Ca ratios from core MD97-2141 [Rosenthal *et al.*, 2003].

[13] Previous studies have shown that Holocene *G. ruber*  $\delta^{18}\text{O}$  values in the southern SCS were much lower than comparable values in the Sulu Sea and the Western Pacific Warm Pool (WPWP) and attributed this isotopic gradient to

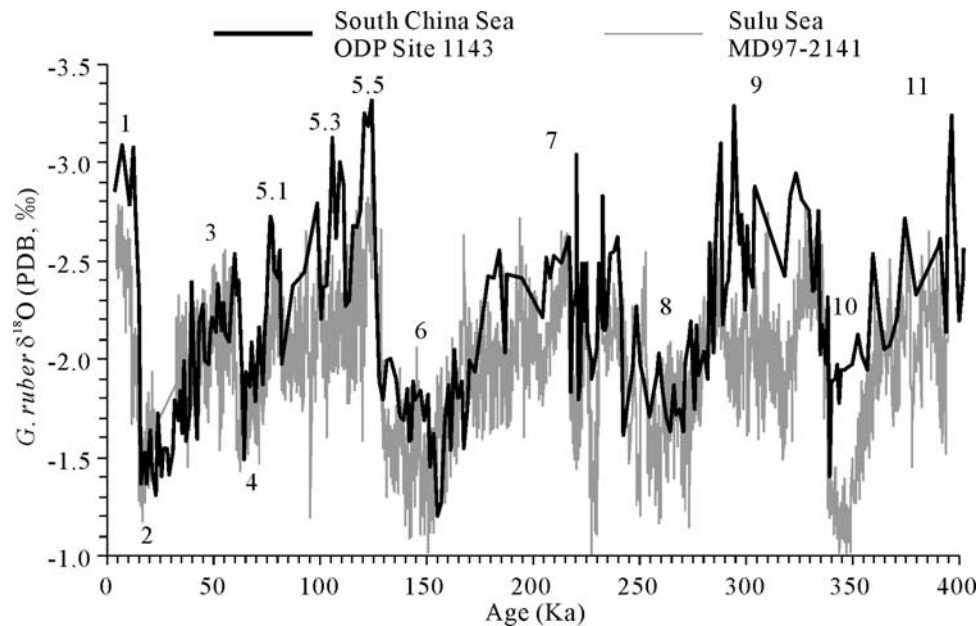


**Figure 4.** Foraminiferal isotopic records from the South China Sea and the Sulu Sea. The thick black line denotes *G. ruber*  $\delta^{18}\text{O}$  of site 1143 in the SCS, and the thin gray line denotes *G. ruber*  $\delta^{18}\text{O}$  of site MD97-2141 in the Sulu Sea [Oppo *et al.*, 2003]. Numbers denote marine isotope stages.

the increasing sea surface salinity (SSS) from the southern SCS through the Sulu Sea and to the WPWP [Steinke *et al.*, 2001; Oppo *et al.*, 2003]. This offset is also clearly visible in the Holocene and other interglacial intervals of site 1143, and is especially significant during the period of MIS 5 (Figure 4). However, *G. ruber*  $\delta^{18}\text{O}$  in the last glacial was also lower in the southern SCS than in the Sulu Sea and WPWP, and was much lower during the periods of MIS 4, 6, 8 and 10 (Figure 4). This finding is different from other studies which have reported that *G. ruber*  $\delta^{18}\text{O}$  values in the southern SCS, Sulu Sea and WPWP were much closer during glacial times, and which have interpreted the absence of significant glacial *G. ruber*  $\delta^{18}\text{O}$  gradients between the SCS and Sulu Sea as due to greater influence of SCS water in the Sulu Sea during glacial times than during interglacial times [Steinke *et al.*, 2001; Oppo *et al.*, 2003]. In the southern SCS, the *G. ruber*  $\delta^{18}\text{O}$  of IMAGES core MD97-2142 also exhibits consistently lower values than those of ODP site 769 and MD97-2141 in the Sulu Sea during both glacial and interglacial times for the past 800 kyr [Wei *et al.*, 2003], and the differences in both glacials and interglacials also reach as much as  $\sim 0.3\text{--}0.5\text{‰}$ . This finding is consistent with our study, and might suggest equivalent influences of the SCS surface water in the Sulu Sea during glacial and interglacial times.

#### 4. Discussion and Conclusions

[14] The LGM cooling relative to the Holocene was  $\sim 3^\circ\text{C}$  on the basis of alkenone thermometry in the SCS [Kienast *et al.*, 2001]. The average glacial/interglacial temperature contrast for the past 470 kyr was  $\sim 3\text{--}4^\circ\text{C}$  on the basis of Mg/Ca ratios from ODP site 806 on the Ontong Java plateau of the open western Pacific [Lea *et al.*, 2000]. Accordingly,

we deduce that decreased SST and an intensified winter monsoon during glacials, which strengthened the thermocline and mixing of the upper ocean in the southern SCS, also deepened the mixed layer in the region as indicated by decreased  $\Delta\delta^{18}\text{O}_{(\text{P-G})}$  values at site 1143.

[15] Similar to the decreased  $\Delta\delta^{18}\text{O}_{(\text{P-G})}$  values, the increased percentage of *P. obliquiloculata* during glacial intervals at site 1143 (Figure 5b) may represent the strengthened winter monsoon. *P. obliquiloculata* is a typical deep water species in the SCS, living in the uppermost part of the thermocline or below the bottom of the mixed layer [Pflaumann and Jian, 1999]. This species dominates the foraminiferal assemblage of deep water species of site 1143 for the past 1.56 Myr. Except for some short intervals, its relative abundance varies from 10% to 55%, with an average of 15% (Figure 5b), and shows distinct glacial/interglacial variations relating more specifically to changes in depth of the mixed layer. Since the sediment trap data (Figures 2a and 2d) reveal high fluxes of *P. obliquiloculata* and *G. ruber* corresponding to the deep winter mixed layer ( $\sim 100$  m), the higher abundances of *P. obliquiloculata* during glacials (Figure 5b) possibly reflect a deeper mixed layer associated with cold intervals. Cooling of the sea surface during glacials may have caused the upper ocean of the SCS to become less stratified and much better ventilated. Under the strong mixing of intensified winter monsoon winds, the mixed layer deepened during glacials for the past 800 kyr. However, relating higher abundances of *P. obliquiloculata* to a deep mixed layer in the southern SCS remains to be confirmed because other studies indicate that deep-dwelling species including *P. obliquiloculata* and *Globorotalia tumida* often dominate the planktonic assemblage during times of a shallower surface mixed layer when the thermocline is located within the photic zone [Bé *et al.*,

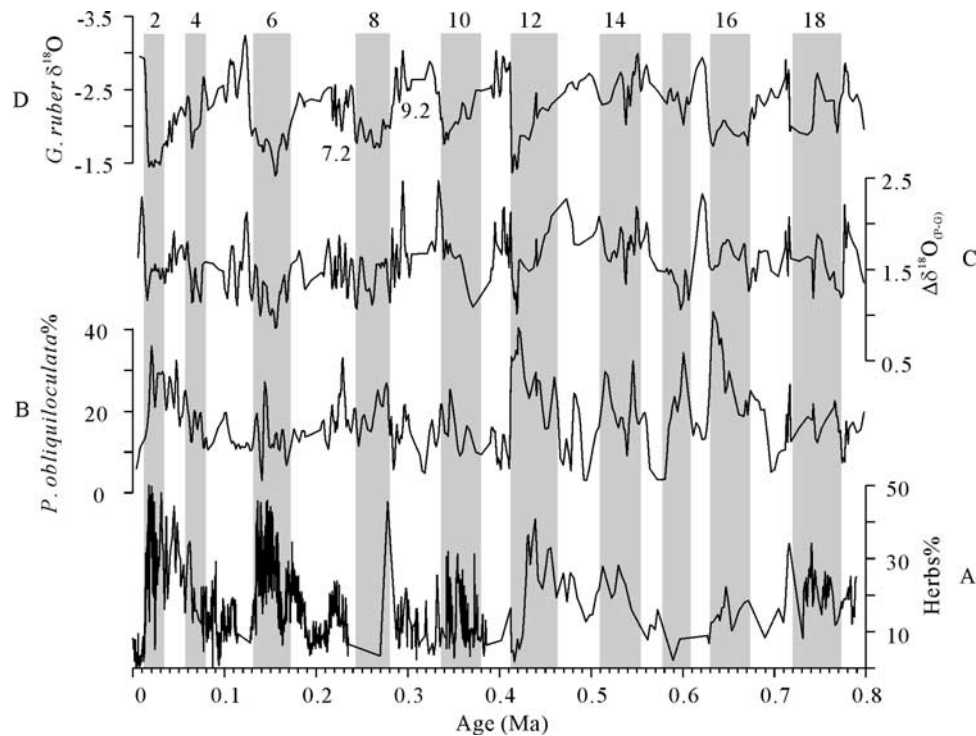


**Figure 5.** East Asian monsoon proxies from the South China Sea: (a) percentage of herbs of site 1144 (0–0.8 Ma) [Sun *et al.*, 2003], (b) percentage of *P. obliquiloculata* of site 1143 (0–0.8 Ma) [Xu *et al.*, 2005], (c)  $\Delta\delta^{18}\text{O}_{(P-G)}$  of site 1143 (PDB, ‰, 3-point Gaussian smoothing, 0–0.8 Ma), and (d) *G. ruber*  $\delta^{18}\text{O}$  of site 1143 (PDB, ‰, 3-point Gaussian smoothing, 0–0.8 Ma). Numbers and shaded bars denote marine isotope stages (cold intervals).

1985]. Therefore processes controlling changes in the relative abundance of *P. obliquiloculata* during glacial intervals may be unique to the southern SCS.

[16] As demonstrated in Figure 5a, changes in the concentration of herb pollen in site 1144 sediments exhibit similar glacial/interglacial changes to that of  $\Delta\delta^{18}\text{O}_{(P-G)}$  and the percent of *P. obliquiloculata* in site 1143. At site 1144 in the northern SCS, herb and *Pinus* pollen comprise the majority of the total pollen. High concentrations of herb pollen but low concentrations of *Pinus* pollen characterize glacials, and vice versa for interglacials [Sun *et al.*, 2003]. The modern pollen distribution in surface sediments of the northern SCS is marked by very high percentages (up to 90% of the total pollen sum) and concentrations of tree pollen, in which *Pinus* is completely dominant [Sun *et al.*, 1999]. The maximum concentration values of tree pollen occur in the northwest adjacent to the convergence of the Bashi and Taiwan Straits, rather than near the estuaries of big rivers, and stretch like a saddle from NE to SW in complete concordance with the direction of the NE winter monsoon and surface currents. Such a distribution pattern implies that tree pollen, especially pine, adapted to wind transport and water flotation, are mainly brought by the NE winter monsoon and wind-driven currents from a large source area, especially south and southeast China [Sun *et al.*, 2003]. During glacials when the continent was drier, herbs replaced pine as the dominant pollen grains transported by winter monsoon winds. Therefore the high concentrations of herbs at site 1144

(Figure 5a) during glacials implies an intensification of the east Asian winter monsoon.

[17] Analogous to higher opal concentrations during winter within the annual cycle as revealed in the sediment trap study in the central SCS (Figure 2c), the opal flux at site 1144 from the northern SCS displays higher concentrations during glacials than during interglacials for the past 1.56 Myr [Li and Wang, 2004]. At a nearby locality, site 1146, siliceous microfossils also show higher abundances and higher accumulation rates during glacials than during interglacials for the past 1.0 Myr [Wang *et al.*, 2003]. The evidence of increased opal flux and siliceous microfossils together implies higher glacial siliceous productivity in the northern SCS caused by strong east Asian winter monsoon winds [Wang *et al.*, 2003]. The intensified east Asian winter monsoon winds during glacials likely enhanced the inflow of upwelled nutrient-rich water through Bashi Strait and the transportation of more eolian dust, resulting in nutrient increases and higher productivity in surface waters of the northern SCS [Wang *et al.*, 1999].

[18] As suggested by Oppo *et al.* [2003], the sea level lowering during glacial times and sea level rise during interglacial times might affect the absolute thermocline depth of the ocean, especially in the western Pacific marginal seas like the Sulu Sea and SCS where there is great influence from ENSO events. Some studies have revealed different influences of ENSO during glacial and interglacial times in the western equatorial Pacific and the

equatorial Indian Ocean [Tudhope et al., 2001; Beaufort et al., 2001], which would consequentially affect the absolute thermocline depth. Further study is needed to clarify how the sea level changes and ENSO variability affect the absolute changes of the mixed layer depth. However, uncertainties concerning the influences from these two factors should not alter the main result of this study, because the  $\delta^{18}\text{O}$  difference used here reflects relative changes of the mixed layer depth or the thermocline depth [Ravelo and Shackleton, 1995] of which the frame of reference is the variable sea surface, not an absolute change from a fixed reference point.

[19] As suggested above, most maritime proxies are not associated with any unique climatic variable but with the integration of several variables, and only the variance held in common among several proxies can be attributed to the variable of interest. This approach is most useful when the proxies are of sufficiently different origin (chemical, physical, biological, isotopic) and from an array of sites such that the variance not held in common is largely independent [Clemens and Prell, 2003]. Although the  $\delta^{18}\text{O}_{\text{(P-G)}}$  and percentage of *P. obliquiloculata* of site 1143, as well as the percentage of herbs and opal flux of site 1144, show many differences in both long- and short-term variations (Figures 5a, 5b, and 5c), they all share common features of strong

glacial/interglacial variations that may have been influenced by strong winter monsoons during glacials. Therefore the main implication of the  $\delta^{18}\text{O}$  differences between *G. ruber* and *P. obliquiloculata* from site 1143 is that an intensified east Asian winter monsoon was the primary factor affecting upper ocean thermal gradient variations, especially the mixed layer depth in the southern SCS during the Quaternary. This conclusion differs from faunal-climate records from the east Pacific where the cool sea surface and the shoaled thermocline are driven by wind-induced upwelling. The hydrologic feature of a deep mixed layer driven by strong winter monsoons in the SCS, as demonstrated by modern observations and comparisons between paleoclimate proxies, seems to be unique in marginal seas where upwelling is weak but the monsoon influence is strong.

[20] **Acknowledgments.** This research used samples provided by the Ocean Drilling Program (ODP). ODP is sponsored by the U.S. National Science Foundation (NSF) and participating countries under management of Joint Oceanographic Institutions (JOI), Inc. The core top samples were obtained during the SONNE-95 cruise and the SONNE -115 cruise. Funding for this research was provided by the NSFC (grants 40476027, 40306011, 4999560, 40321603, and 40331002) and NKBRFSF (grant G2000078500). Michael Sarnthein is acknowledged for his supply of the core top data.

## References

- Bé, A. W. H., J. K. B. Bishop, M. S. Swerdlove, and W. D. Gardner (1985), Standing stock, vertical distribution and flux of planktonic foraminifera in the Panama Basin, *Mar. Micropaleontol.*, **9**, 307–333.
- Beaufort, L., T. de Garidel-Thoron, A. C. Mix, and N. G. Pisias (2001), ENSO-like forcing on oceanic primary production during the late Pleistocene, *Science*, **293**, 2440–2444.
- Billups, K., A. C. Ravelo, J. C. Zachos, and R. D. Norris (1999), Link between oceanic heat transport, thermohaline circulation, and the intertropical convergence zone in the early Pliocene Atlantic, *Geology*, **27**, 319–322.
- Clemens, S., and W. Prell (2003), A 350,000 year summer-monsoon multi-proxy stack from the Owen Ridge, northern Arabian Sea, *Mar. Geol.*, **201**, 35–51.
- Ding, Z. L., N. W. Rutter, J. T. Han, and T. S. Liu (1992), A coupled environmental system formed at about 2.5 Ma over east Asia, *Palaeogeogr. Palaeoclimatol. Palaeoecol.*, **94**, 223–242.
- Grothmann, A. (1996), *Rezente Verbreitungsmuster vulkanischer, terrigener und biogener Komponenten und stabiler Kohlenstoff- und Sauerstoff-Isotope in Sedimenten der Südkina-See*, M.Sc. thesis, Kiel Univ., Kiel, Germany.
- Hemleben, C., M. Spindler, and O. R. Anderson (1989), *Modern Planktonic Foraminifera*, Springer, New York.
- Kienast, M., S. Steinke, K. Statteger, and S. E. Calvert (2001), Synchronous tropical South China Sea SST change and Greenland warming during deglaciation, *Science*, **291**, 2132–2134.
- Laskar, J. (1990), The chaotic motion of the solar system: A numerical estimate of the size of the chaotic zones, *Icarus*, **88**, 266–291.
- Lea, D. W., D. K. Pak, and H. J. Spero (2000), Climate impact of Late Quaternary equatorial Pacific sea surface temperature variation, *Science*, **289**, 1719–1724.
- Levitus, S. (1982), *Climatological Atlas of the World Ocean*, NOAA Prof. Pap., **13**, 173 pp.
- Levitus, S., and T. P. Boyer (1994), *World Ocean Atlas 1994*, vol. 4, *Temperature*, NOAA Atlas NESDIS 4, 129 pp., NOAA, Silver Spring, Md.
- Li, J., and R. J. Wang (2004), Paleoproductivity variability of the northern South China Sea during the past 1 Ma: The opal record from ODP site 1144 (in Chinese with English abstract), *Acta Geol. Sin.*, **78**(2), 228–233.
- Linsley, B. (1996), Oxygen-isotope record of sea level and climate variations in the Sulu Sea over the past 150,000 years, *Nature*, **380**, 234–237.
- Oppo, D. W., B. K. Linsley, Y. Rosenthal, S. Dannenmann, and L. Beaufort (2003), Orbital and suborbital climate variability in the Sulu Sea, western tropical Pacific, *Geochem. Geophys. Geosyst.*, **4**(1), 1003, doi:10.1029/2001GC000260.
- Pflaumann, U., and Z. Jian (1999), Modern distribution patterns of planktonic foraminifera in the South China Sea and western Pacific: A new transfer technique to estimate regional sea-surface temperatures, *Mar. Geol.*, **156**, 41–83.
- Porter, S. C., and Z. An (1995), Correlation between climate events in the North Atlantic and China during the last glaciation, *Nature*, **375**, 305–308.
- Porter, S. C., Z. S. An, and H. B. Zheng (1992), Cyclic Quaternary alleviation and terracing in a nonglaciated drainage basin on the north flank of Qingling Shan, central China, *Quat. Res.*, **38**, 157–169.
- Ravelo, A., and N. J. Shackleton (1995), Evidence for surface-water circulation changes at site 851 in the eastern tropical Pacific Ocean, *Proc. Ocean Drill. Program Sci. Results*, **138**, 503–514.
- Rosenthal, Y., D. W. Oppo, and B. K. Linsley (2003), The amplitude and phasing of climate change during the last deglaciation in the Sulu Sea, western equatorial Pacific, *Geophys. Res. Lett.*, **30**(8), 1428, doi:10.1029/2002GL016612.
- Sarnthein, M., U. Pflaumann, P. X. Wang, and H. K. Wong (1994), Preliminary report on SONNE-95 cruise ‘Monitor Monsoon’ to the South China Sea, *Ber. Rep. Geol. Paläontol. Inst. Univ. Kiel* **68**, 225 pp., Kiel Univ., Kiel, Germany.
- Shaw, P. T. (1996), Winter upwelling off Luzon in the northeastern South China Sea, *J. Geophys. Res.*, **101**, 16,435–16,448.
- Sigman, D. M., S. L. Jaccard, and G. H. Haug (2004), Polar ocean stratification in a cold climate, *Nature*, **428**, 59–63.
- Statteger, K., et al. (1997), Cruise report SONNE 115 SUNDAFLUT: Sequence stratigraphy, late Pleistocene-Holocene sea level fluctuations and high resolution record of the post-Pleistocene transgression on the Sunda Shelf, *Ber. Rep. Geol. Paläontol. Inst. Univ. Kiel* **86**, 211 pp., Kiel Univ., Kiel, Germany.
- Steinke, S., M. Kienast, U. Pflaumann, M. Weinelt, and K. Statteger (2001), A high resolution sea-surface temperature record from the tropical South China Sea (16,500–3000 B. P.), *Quat. Res.*, **5**, 353–362.
- Sun, X., X. Li, and H.-J. Beug (1999), Pollen distribution in hemipelagic surface sediments of the South China Sea and its relation to modern vegetation distribution, *Mar. Geol.*, **156**, 211–226.

- Sun, X. J., Y. L. Luo, F. Huang, J. Tian, and P. X. Wang (2003), Deep-sea pollen from the South China Sea: Pleistocene indicators of east Asian monsoon, *Mar. Geol.*, *201*, 97–118.
- Tian, J., P. X. Wang, X. R. Chen, and Q. Y. Li (2002), Astronomically tuned Plio-Pleistocene benthic  $\delta^{18}\text{O}$  records from South China Sea and Atlantic-Pacific comparison, *Earth Planet. Sci. Lett.*, *203*, 1015–1029.
- Tian, J., P. X. Wang, and X. R. Chen (2003), Development of the east Asian monsoon and Northern Hemisphere glaciation: Oxygen isotope records from the South China Sea, *Quat. Sci. Rev.*, *23*, 2007–2016.
- Tudhope, A. W., C. P. Chilcott, M. T. McCulloch, E. R. Cook, J. Chappell, R. M. Ellam, D. W. Lea, and J. M. Lough (2001), Variability in the El Niño–Southern Oscillation through a glacial-interglacial cycle, *Science*, *291*, 1511–1577.
- Wang, D., Y. Du, and P. Shi (2001), Evidence for thermocline ventilation in the South China Sea in winter, *Chin. Sci. Bull.*, *46*(9), 774–778.
- Wang, L., M. Samthein, H. Erlenkeuser, J. Grimalt, P. Grootes, S. Heilig, E. Ivanova, M. Kienast, C. Pelejero, and U. Pflaumann (1999), East Asian monsoon climate during the Late Pleistocene: High-resolution sediment records from the South China Sea, *Mar. Geol.*, *156*, 245–284.
- Wang, R., S. Clemens, B. Huang, and M. Chen (2003), Quaternary paleoceanographic changes in the northern South China Sea (ODP site 1146), radiolarian evidence, *J. Quat. Sci.*, *18*(8), 745–756.
- Wei, K. Y., T. C. Chiu, and Y. G. Chen (2003), Toward establishing a maritime proxy record of the east Asian summer monsoons for the late Quaternary, *Mar. Geol.*, *201*, 67–79.
- Wiesner, M. G., L. F. Zheng, and H. K. Wong (1996), *Fluxes of Particulate Matter in the South China Sea*, pp. 91–154, John Wiley, Hoboken, N. J.
- Wyrski, K. (1961), Scientific results of marine investigations of the South China Sea and Gulf of Thailand 1959 ~ 1961, *NAGA Rep.* *2*, pp. 164–169, Scripps Inst. of Oceanogr., Univ. of Calif., San Diego, Calif.
- Xu, J., P. X. Wang, B. Q. Huang, Q. Y. Li, and Z. M. Jian (2005), Response of planktonic foraminifera to glacial cycles: Mid-Pleistocene change in the southern South China Sea, *Mar. Micropaleontol.*, *54*, 89–105.
- Yang, H. J., and Q. Y. Liu (1998), A summary on ocean circulation study of the South China Sea (in Chinese with English abstract), *Adv. Earth Sci.*, *13*(4), 364–368.
- 
- R. Chen, Key Laboratory of Submarine Geosciences of State Oceanic Administration, Hangzhou 310012, China.
- X. Cheng, J. Tian, and P. Wang, State Key Laboratory of Marine Geology, Tongji University, Shanghai 200092, China. (ian.tianjun@263.net)